

# EarthCARE ATLID L2 products in comparison with ground-based lidar retrievals of aerosols and cirrus clouds at El Arenosillo station (southwestern Iberian Peninsula): First one year-round validation results

Noé Rodríguez-Rivas<sup>1</sup> ([nrodriv@inta.es](mailto:nrodriv@inta.es)), Jennifer López-Viejobueno<sup>1</sup>, Eduardo Leante-García<sup>2</sup>,

Laura Gómez-Martín<sup>1</sup>, Juan Luis Guerrero-Rascado<sup>3,4</sup>, and Carmen Córdoba-Jabonero<sup>1</sup> ([cordoba@inta.es](mailto:cordoba@inta.es))

<sup>1</sup>Instituto Nacional de Técnica Aeroespacial (INTA), Atmospheric Research and Instrumentation Branch, Torrejón de Ardoz (Madrid), Spain

<sup>2</sup>Universidad Complutense de Madrid (UCM), Madrid, Spain

<sup>3</sup>Applied Physics Department, University of Granada (UGR), Granada, Spain

<sup>4</sup>Andalusian Institute for Earth System Research (IISTA-CEAMA), University of Granada (UGR), Granada, Spain



**Aim.** Introducing the first one year-round results obtained from the intercomparison of the EarthCARE (EC) ATLID L2 products with ground-based (GB) lidar observations carried out at the MPLNET El Arenosillo station (ARN; 37.1°N, 6.7°W), which is located at the southwest of the Iberian Peninsula. A comprehensive statistical validation is presented regarding: 1) target classification (ATL-TC) depending on the EC baseline; and 2) optical properties (ATL-EBD): the particle backscattering coefficient ( $\beta_p$ ) and the particle linear depolarization ratio ( $\delta_p$ ) in aerosol and ice clouds (cirrus) scenarios. It should be taken into account that the comparison of EC optical properties ( $\beta_p$  and  $\delta_p$ ) with GB lidar retrievals in aerosol scenarios could reflect, additionally to other issues, the wavelength difference between ATLID (355 nm) and P-MPL (532 nm). This is not the case for cirrus clouds, as their optical properties exhibit little to no wavelength dependence between 355 and 532 nm. The analysis has been performed in the context of the EC ATLID Validation Team.

## Ground-based lidar

### Polarized Micro-Pulse Lidar (P-MPL):

- Elastic system: 532 nm, 2500 Hz, 5-7  $\mu$ J
- Depolarization (co- and cross-channels)
- Acquisition settings: 75 m / 1 min



El Arenosillo station (ARN): 37.1°N 6.7°W, 59 m asl  
Micro Pulse Lidar Network (MPLNET), <https://mplnet.gsfc.nasa.gov>

## EC overpasses over ARN



Condition:  
< 100 km radius  
around the station

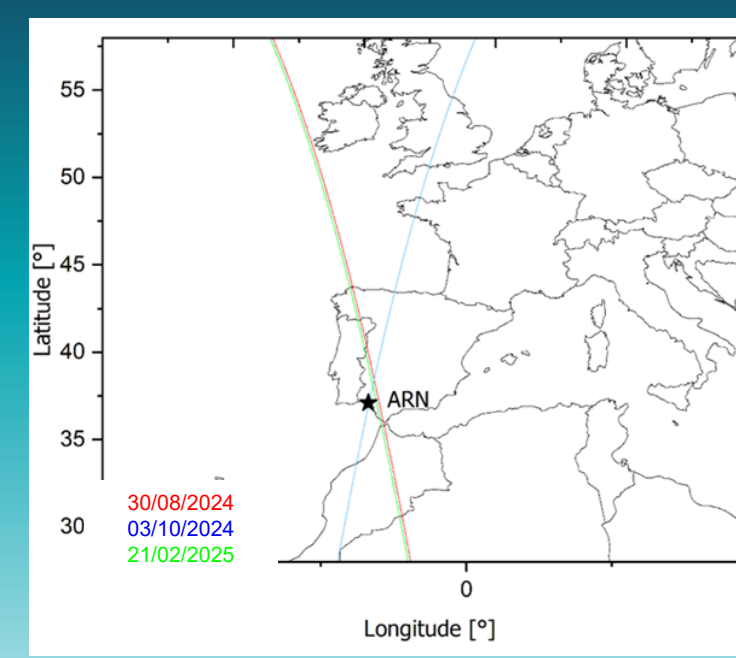
Period: 1 August 2024 - 31 July 2025  
(55 overpasses)

### Aerosol scenarios:

- Altitude detection: 0.1-8.0 km
- ATLID profiles at the minimum distance
- Retrieval (good weather, no instrumental failure): 45 % (25 cases)

### Ice cloud scenarios:

- Altitude detection: 6.0-15.0 km height
- ATLID profiles at the minimum distance
- Cirrus detected: 6 cases



## Methodology

### Space-borne (EC) ATLID (355 nm)

- ATL-EBD:  $\beta_p$ ,  $\delta_p$ , and QS (quality data status)
- ATL-TC: target classification with baselines: BA and AX (AC, AD, AE, AD)
- Vertical res.: 103 m (< 20 km)
- Horizontal res.: 1 km

### Ground-based (GB) P-MPL (532 nm)

- range-corrected signal (RCS)
- volume depolarization ratio (VDR)
- Averaged NRB profiles around  $\pm 90$  minutes of the closest EC overpass: three 1-h profiles
- Vertical res.: 75 m
- Integrating time: 1 min
- Inversion methods: [4, 5] for clouds, and [6] for aerosol

### Statistical parameters for validation:

Mean Factorial Bias (MFB, %):  $MFB = \frac{1}{N} \sum_{i=1}^N 2 \cdot \frac{\bar{X}_{S_i} - \bar{X}_{O_i}}{\bar{X}_{S_i} + \bar{X}_{O_i}}$  S = EC ATLID, O = GB lidar

- Coefficient of Determination (CC: correlation analysis)

## RESULTS AND DISCUSSION

### ATL-TC: EC baseline

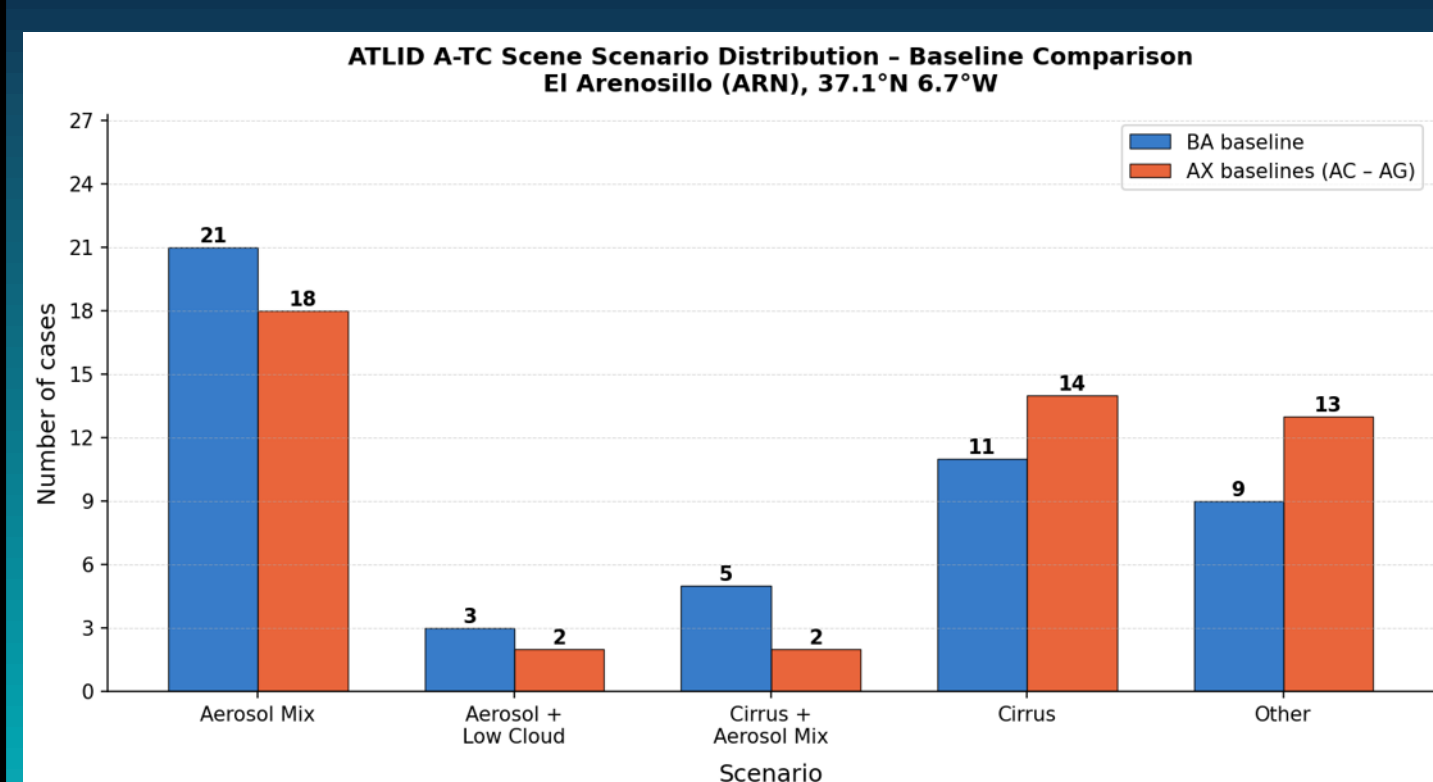


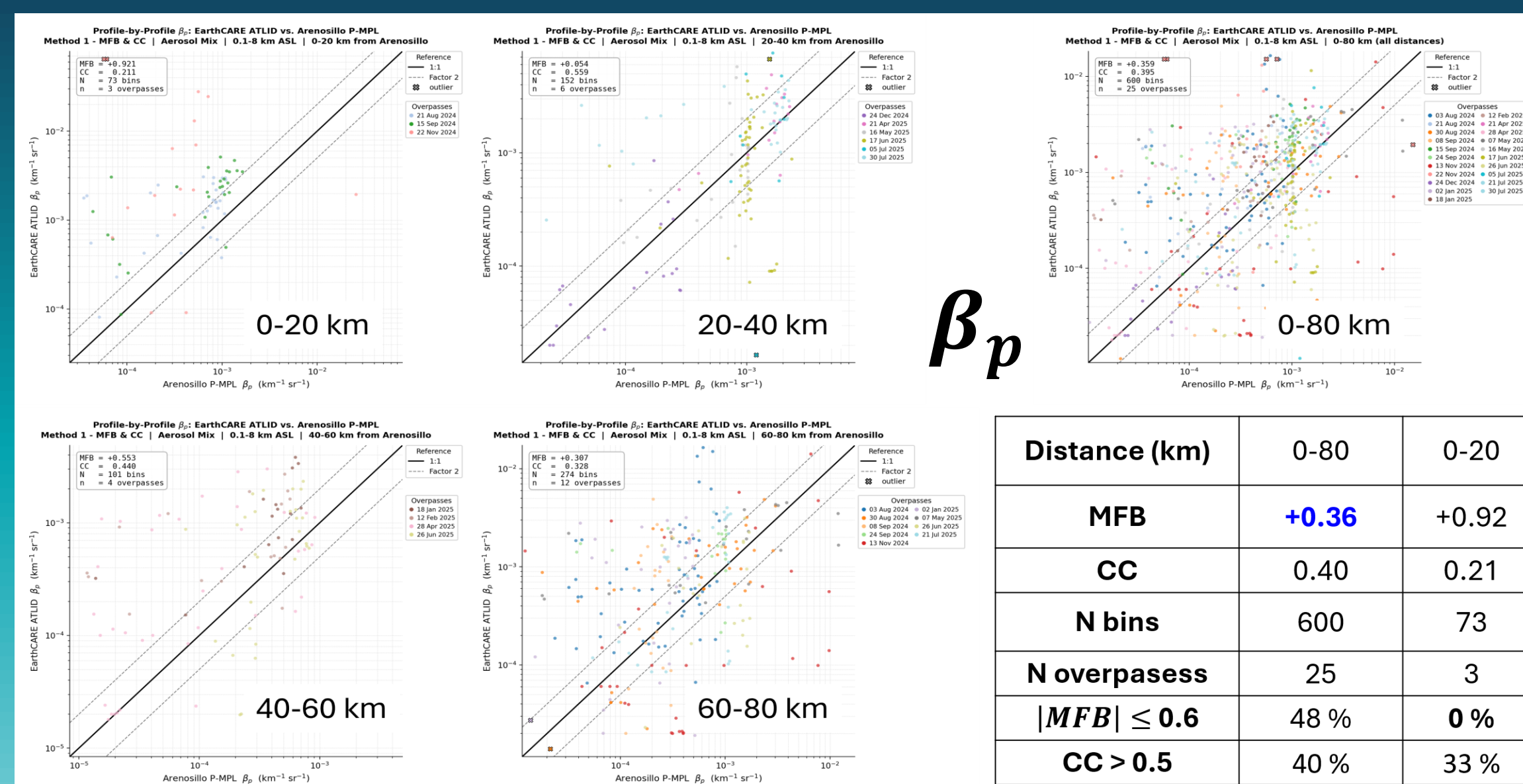
Figure 1. Target Classification (TC) reported by EC (in percentage of total simultaneous cases = 49) depending on the EC baseline: BA (blue) and AX (AC-AF; red).

### BA vs. AX baselines:

- BA baseline shows systematically higher sensitivity to aerosols: accounts ~10-13 vertical bins while AX detects only 7-9 bins for the same overpass.
- This translates into 14 TC misclassifications out of 49 cases (~28.6 %).
- BA accounts aerosol layers that AX missed: three cirrus cases observed in AX correspond to 'Cirrus + Aerosol Mix' in BA.
- Three cases classified as 'Other' in AX are correctly identified as 'Aerosol Mix' or 'Aerosol + Low Cloud' in BA.
- BA baseline detects 21 'Aerosol mix' cases vs. 18 in AX, and 5 'Cirrus-Aerosol Mix' vs. 2 in AX.

### ATL-EBD (BA): $\beta_p$ and $\delta_p$

#### Aerosol scenarios

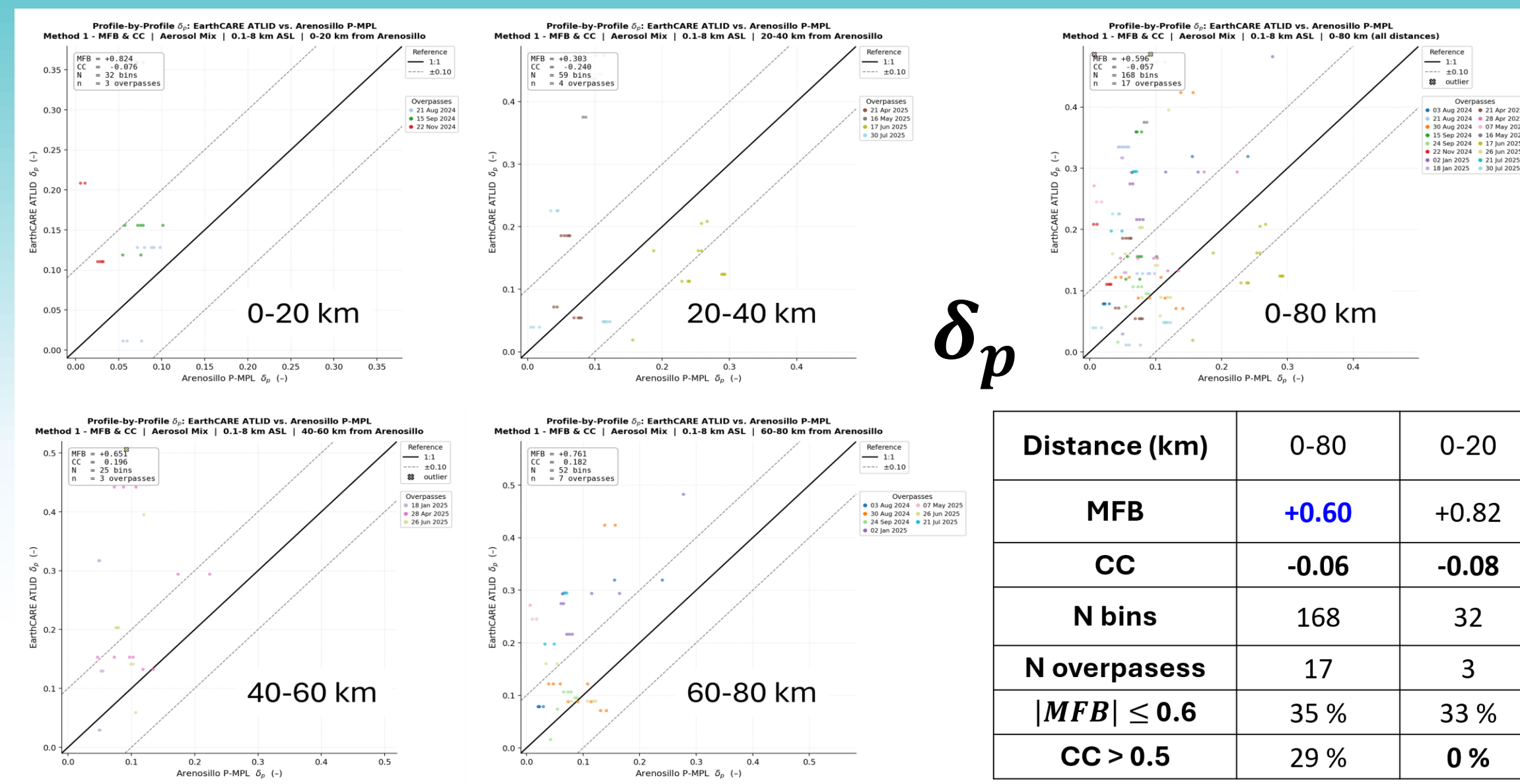


$\beta_p$

Distance (km)	0-80	0-20	20-40	40-60	60-80
MFB	+0.36	+0.92	+0.05	+0.55	+0.31
CC	0.40	0.21	0.56	0.44	0.33
N bins	600	73	152	101	274
N overpasses	25	3	6	4	12
MFB  $\leq$ 0.6	48 %	0 %	83 %	25 %	50 %
CC > 0.5	40 %	33 %	67 %	50 %	25 %

Figure 2a.

'Aerosol Mix': 25 cases. Particle backscatter coefficient ( $\beta_p$ ;  $\text{km}^{-1} \text{sr}^{-1}$ ) comparison depending on the distance from ARN to the EC overpass. Vertical range: 0.1-8.0 km height.



$\delta_p$

Distance (km)	0-80	0-20	20-40	40-60	60-80
MFB	+0.60	+0.82	+0.30	+0.65	+0.76
CC	-0.06	-0.08	-0.24	0.20	0.18
N bins	168	32	59	25	52
N overpasses	17	3	4	3	7
MFB  $\leq$ 0.6	35 %	33 %	25 %	33 %	43 %
CC > 0.5	29 %	0 %	25 %	0 %	57 %

Figure 2b.

'Aerosol Mix': 17 cases. Particle linear depolarization ratio ( $\delta_p$ ) comparison depending on the distance from ARN to the EC overpass. Vertical range: 0.1-8.0 km height.

#### Cirrus cloud scenarios

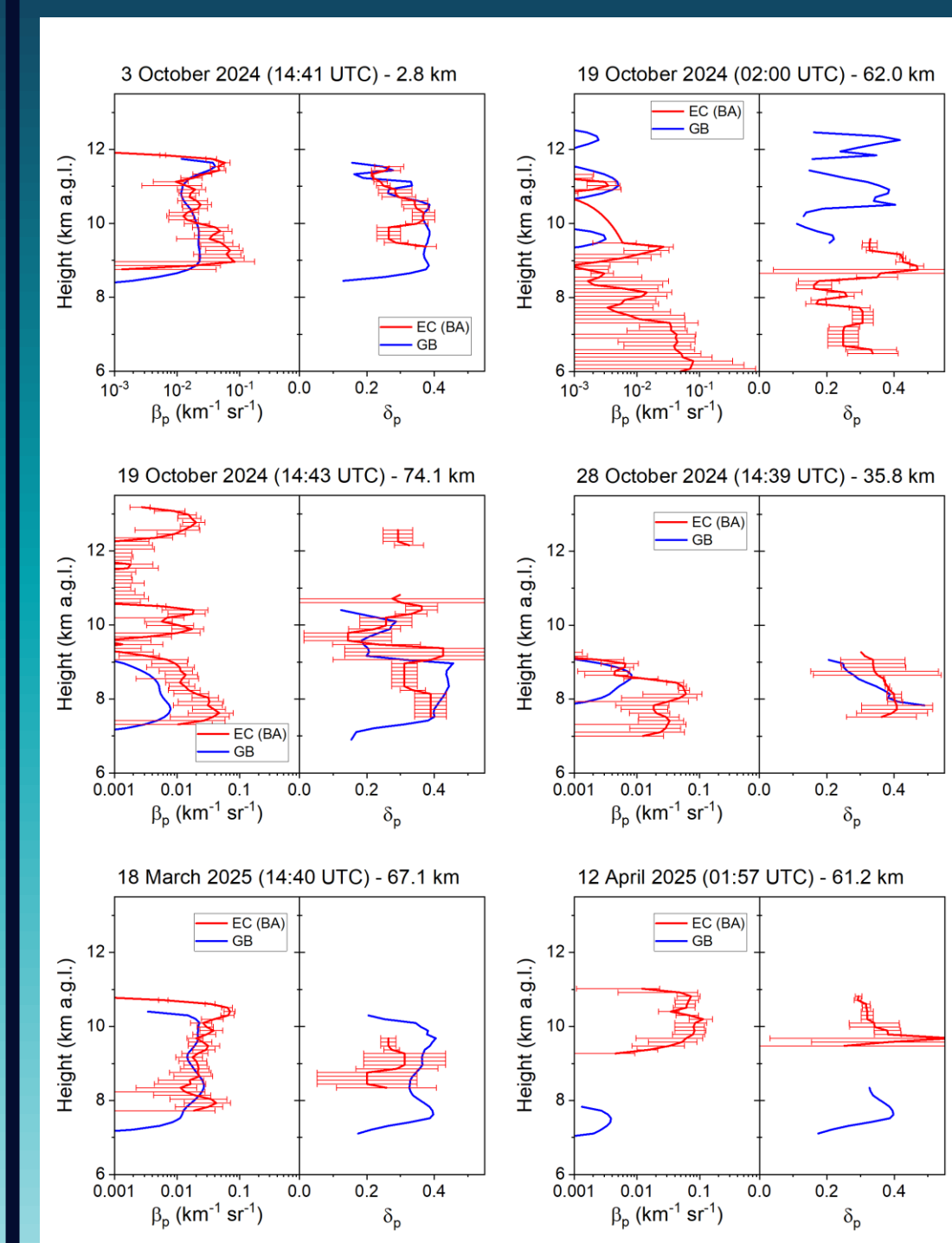


Figure 3.

Cirrus cases (6). (Left panels) Particle backscatter coefficient ( $\beta_p$ ;  $\text{km}^{-1} \text{sr}^{-1}$ ), and (Right panels) particle linear depolarization ratio ( $\delta_p$ ) comparison (EC vs. GB profiles). Day, time and distance from ARN to the EC overpass are included at the top. Vertical range: 6.0-15.0 km height.

Case	03/10 2024 14:41 UTC	19/10 2024 02:00 UTC	19/10 2024 14:43 UTC	28/10 2024 14:39 UTC	18/03 2025 14:40 UTC	12/04 2025 01:57 UTC
Distance (km)	2.8	62.0	74.1	35.8	67.1	61.2
$\beta_p$						
MFB	+0.33	+0.25	+1.27	+1.19	+0.28	---
CC	0.97	0.93	0.96	0.87	0.97	---
slope	0.92	0.88	0.71	0.62	0.90	---
N bins	30	30	29	18	27	0
$\delta_p$						
MFB	-0.10	+0.42	-0.01	+0.15	-0.33	---
CC	0.97	1.00	0.89	0.97	0.80	---
slope	0.88	1.53	0.90	1.09	0.73	---
N bins	22	2	29	13	14	0

### Main Remarks:

- The EC BA dataset shows evidently an improvement with respect to previous baselines (AX) in target classification (TC). However, depolarization concerns are still to be solved; consequently, this affects to the EC TC (i.e., ATL-TC products), being more noticeable in aerosol scenarios than for ice clouds.
- Aerosol cases ( $\beta_p$  //  $\delta_p$ ):
  - Global MFB = +0.36 // +0.60: ATLID overestimation w.r.t. GB lidar, ~ 36% // ~ 60% on average; 21/25 // 16/17 cases (84% // 94%) show positive MFB. 48 % // 35 % out of cases (12/25 // 6/17) fulfil an acceptable MFB criterion ( $|MFB| \leq 0.6$ ).
  - CC = 0.40 // 0.06: moderate // weak agreement in vertical structure overall. 40 % // 29 % out of cases (10/25 // 5/17) fulfil a good CC criterion ( $CC \geq 0.5$ ).
  - Systematic positive MFB: for  $\beta_p$  it can be explained by the wavelength difference: ATLID at 355 nm vs. P-MPL at 532 nm, but for  $\delta_p$  it cannot be explained by the wavelength difference only, in addition to likely depolarization retrieval/calibration issues.
- Cirrus cases ( $\beta_p$  and  $\delta_p$ ):
  - The closest case (03 October 2024 at 2.8 km distance) show the best agreement in the three statistical parameters. One case (12 April 2025) is discarded, as there is no coincidence at the same altitudes.
  - MFB values are all positive for  $\beta_p$  (ATLID overestimation w.r.t. GB lidar), but not for  $\delta_p$  (depending on the cirrus case). 3/5 ( $\beta_p$ ) and 5/5 ( $\delta_p$ ) cases fulfil an acceptable MFB criterion ( $|MFB| \leq 0.6$ ).
  - For both  $\beta_p$  and  $\delta_p$ : CC > 0.80 in all the cases, and the slope values are close to 1 in the most cases.
  - Overall, a good agreement is achieved in vertical structure for both  $\beta_p$  and  $\delta_p$ .

References: [1] Donovan et al., Atmos. Meas. Tech., 17, 5301-5340, 2024. [2] Campbell et al., J. Atmos. Oceanic Technol., 19, 431-442, 2002. [3] Welton and Campbell, J. Atmos. Oceanic Technol., 19, 2089-2094, 2022. [4] Córdoba-Jabonero et al., Atmos. Res., 183, 151-165, 2017. [5] Córdoba-Jabonero et al., Atmos. Res., 246, 105095, 2020. [6] Córdoba-Jabonero et al., Atmos. Meas. Technol., 11, 4775-4795, 2018.

Acknowledgments. This work has received funding from the European Union's Horizon 2020 research and innovation programme through the ATMO-ACCESS Integrating Activity under GA N° 101008004. It is also supported by the Spanish Agencia Estatal de Investigación (AEI)-Ministerio de Ciencia, Innovación y Universidades (MICIU) (grant PID2023-151666NB-I00, and research mobility PRX24/00599). The MPLNET project is funded by the NASA Radiation Sciences Program and Earth Observing System. The authors acknowledge the PI and technical staff of the ARN station for maintenance support of the P-MPL system.

